PRESSURE DROP IN THE PNEUMATIC CONVEYANCE OF GRANULAR SOLIDS THROUGH A PIPE

TOKIO UEMATSU

Dept. Mech. Engineering, Osaka University, Osaka, Japan

Synopsis—The pressure drop in the flow of a pneumatic conveyor is experimentally treated. From the experimental results on a straight pipe and pipe bend an empirical formula for the additional pressure drop due to solids is obtained.

LIST OF SYMBOLS

The following nomenclature is used in this paper.

Δp	Total pressure drop in straight pipe
Δp_a	Pressure drop in the flow of air through a straight pipe
Δp_s	Pressure drop due to solids in a straight pipe
$\Delta p'$	Total pressure drop in pipe bend
Δp_b	Pressure drop in the flow of air through a pipe bend
Δp_0	Pressure drop in the straight pipe preceding pipe bend
Δp_u	Pressure drop in the straight pipe following pipe bend
Δp_k	Pressure drop between the inlet and exit of pipe bend
λ	Coefficient of fluid friction
λ_s	Coefficient defined by Eq. (4)
ζ'	Coefficient in reference to $\Delta p'$
ζ_b	Coefficient in reference to Δp_b
ζ_s	Coefficient defined by Eq. (17)
l	Length of pipe
d	Internal diameter of pipe
r	Internal radius of pipe
R	Radius of curvature
ϱ	Specific mass of air
u	Mean velocity of air

$Re = ud/\nu$	Reynolds number
ν	Kinematic viscosity of air
μ	Weight ratio of solids to air in flow
θ	Angle of direction change
x	Distance measured from first pressure take off (see Fig. 2)
p_0	Pressure at $x = 0$
p	Pressure on the pipe wall

1. INTRODUCTION

Pneumatic conveyors have been used in transporting granular solids for many years. Many investigators have studied the problem since the end of the Second World War. The fundamental step in the calculation for the design of a conveyor pipe-line is the correct estimation of pressure drop along the pipe length. The determination of the law relating to this is therefore the main subject of many papers on pneumatic conveyance. The author deals in this paper with the pressure drop in a horizontal pneumatic conveyance including a pipe bend.

From measurements made, an empirical formula is desired to express the pressure drop under these conditions.

2. EXPERIMENTAL APPARATUS

The arrangement of the straight pipe is illustrated in Fig. 1. The diameter of holes from 1 to 10, from which the pressure is led to

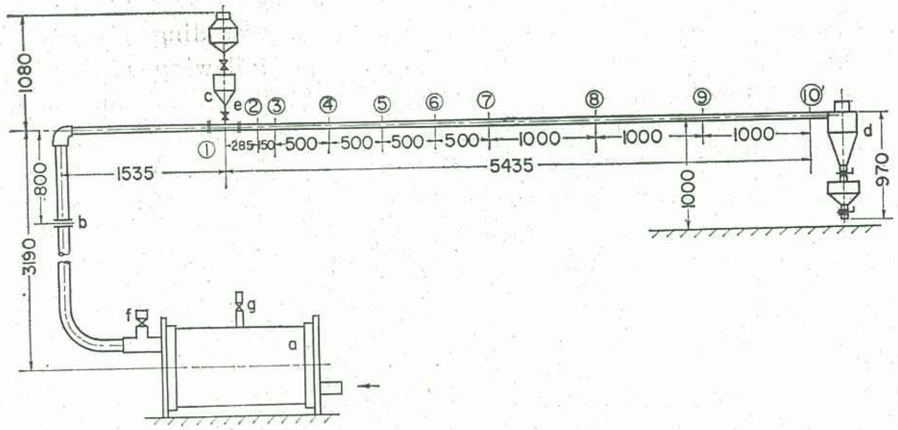

FIG. 1. Experimental apparatus. *a:* air tank, *b:* orifice, *c:* hopper, *d:* cyclone, *e:* cock, *f, g:* valve.

each manometer, was 1 mm. The characteristics of materials used in this experiment are shown in Table 1. The pipe bends used are found in Table 2 and one of them is shown in Fig. 2. The straight

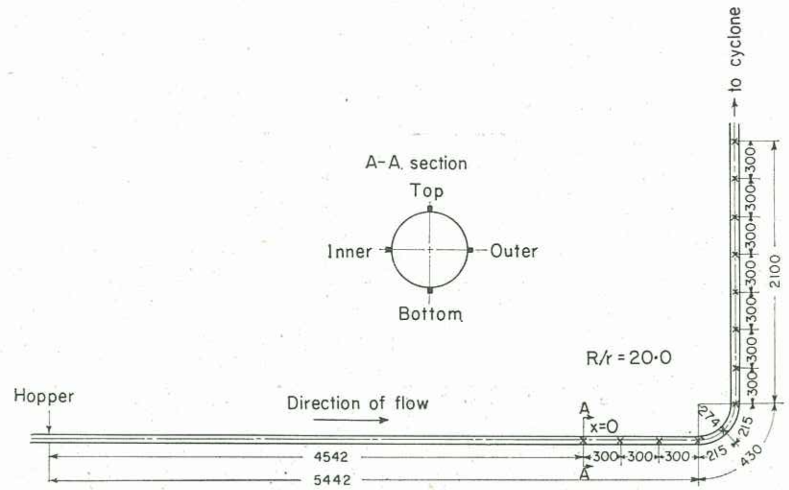

FIG. 2. One of the pipe bends used in the experiment.

pipes of sufficient length were connected upstream and downstream of the bend. Each manometer connection at the pipes consists of four holes, 1 mm diameter, drilled at 90-degree intervals in the circumference as shown in Fig. 2.

TABLE 1. CHARACTERISTICS OF MATERIALS USED IN THE EXPERIMENT

Material	Mean diameter (mm)	Specific weight (kg/m³)
Mustard seed	0·97	1240
Rape seed	1·53	1090
Millet seed	1·63	1090
Sesame	1·63	1070
Hemp seed	3·47	915
Polyethylene	2·95	925
Synthetic resin	3·46	928
Wheat	4·02	1380
Soybean	8·52	1220

TABLE 2. PIPE BENDS

θ deg	$R/[a:r]$
90	20·0
	12·0
180	19·4
	11·5

3. PRESSURE DROP IN A STRAIGHT PIPE

The pressure drop during the conveying of solids consists of various factors, such as friction of air on pipe wall, friction of air on solid (dependent upon the relative velocity of air and solid), friction of solid on pipe wall, and collision of solid particles against each other and against the pipe wall. It is difficult, however, to divide the total pressure drop under consideration into all these factors. An assumption is made, therefore, that the total pressure drop in a straight pipe consists of pressure drop in the flow of air through a straight pipe and that due to solids. Under this assumption the expression is given

$$\Delta p = \Delta p_a + \Delta p_s \tag{1}$$

(a) *Coefficient of Fluid Friction*

In order to know correctly the additional pressure drop due to solids, it is necessary to determine the coefficient of fluid friction, when air alone moves along a pipe. The pressure drop in the flow of air through a straight pipe is given in the following basic equation

$$\Delta p_a = \lambda \frac{l}{d} \frac{\varrho}{2} u^2 \tag{2}$$

The coefficient of fluid friction for the straight pipe obtained from measurements is shown plotted against the Reynolds number

in Fig. 3, which shows that the results are in close agreement with the Blasius formula

$$\lambda = 0{\cdot}3164/Re^{\frac{1}{4}} \tag{3}$$

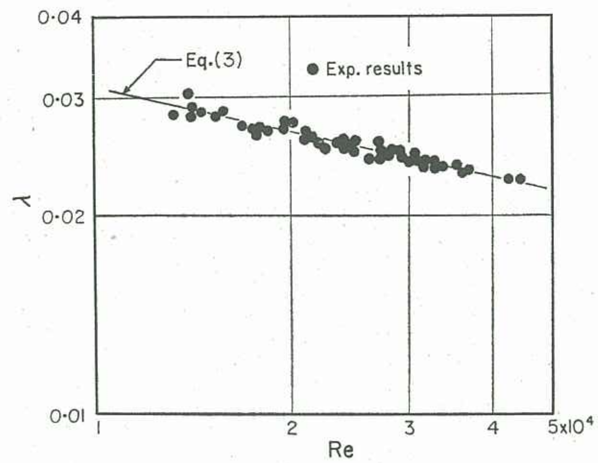

FIG. 3. Comparison of experimental results with the Blasius formula.

(b) *Pressure Drop due to Solids in a Straight Pipe*

The pressure drop due to solids in a straight pipe, with which the author deals here, is uninfluenced by the acceleration of the solids after the feeder, i.e. in other words the steady state has been reached. Putting the pressure drop

$$\Delta p_s = \lambda_s \frac{l}{d} \frac{\varrho}{2} u^2 \tag{4}$$

only the coefficient λ_s is to be known in order to obtain Δp_s. By making use of the total pressure drop Δp, the shearing stress τ_0 at pipe wall is calculated from

$$\tau_0 = \frac{\Delta p}{l} \frac{[a:r]}{2} \tag{5}$$

from which the friction velocity v_* is obtained

$$v_* = \sqrt{(\tau_0/\varrho)} \tag{6}$$

The velocity ratio u/v_* is plotted against μ in Fig. 4, which shows the relation between u/v_* and μ is independent of the characteristics of solids and is expressed by a straight line. In the case of $\mu = 0$ the following relation is given

$$u/v_* = \sqrt{(8/\lambda)} \tag{7}$$

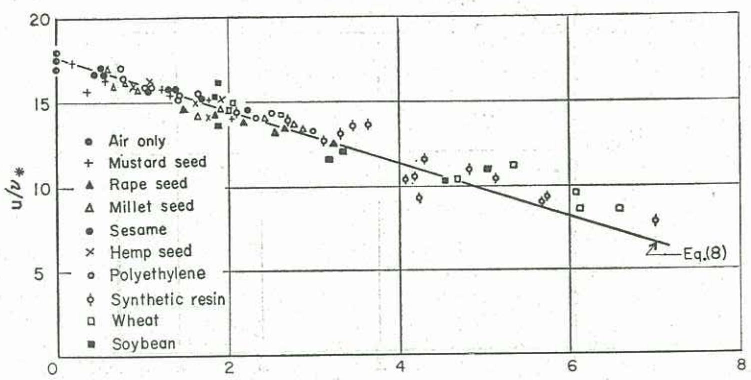

FIG. 4. Relation of u/v_* vs. μ.

Using this equation the relation in Fig. 4 is expressed by

$$u/v_* = \sqrt{[(8/\lambda) - 1{\cdot}72\ \mu]} \tag{8}$$

From (1), (2) and (4) it follows that

$$\Delta p = (\lambda + \lambda_s)\frac{l}{d}\frac{\varrho}{2}u^2 \tag{9}$$

and hence

$$\frac{\Delta p}{l} = \frac{\lambda}{d}\frac{\varrho}{2}u^2\left(1 + \frac{\lambda_s}{\lambda}\right) \tag{10}$$

From (5), (6) and (10) the relation

$$\tau_0 = \frac{\lambda}{8}\varrho u^2\left(1 + \frac{\lambda_s}{\lambda}\right) \tag{11}$$

is given. Substituting (8) into (11) the coefficient λ_s may be expressed in the form

$$\lambda_s = \frac{8}{[\sqrt{(8|\lambda)} - 1{\cdot}72\mu]^2} - \lambda \tag{12}$$

By this formula the pressure drop due to solids is easily obtained, if only λ and μ are known. By substituting (12) into (9) the total pressure drop is expressed in the form

$$\Delta p = \frac{8}{[\sqrt{(8/\lambda)} - 1{\cdot}72\mu]^2}\frac{l}{d}\frac{\varrho}{2}u^2 \tag{13}$$

In order to deduce (12) or (13) the effect of solids upon the pressure drop is considered by introducing both the weight ratio of solids to air in the flow and the friction velocity.

4. PRESSURE DROP IN PIPE BEND

A typical example of the curves of the measured pressure distribution along a pipe bend including straight pipes preceding and following it is shown in Figs. 5 and 6, where the experimental

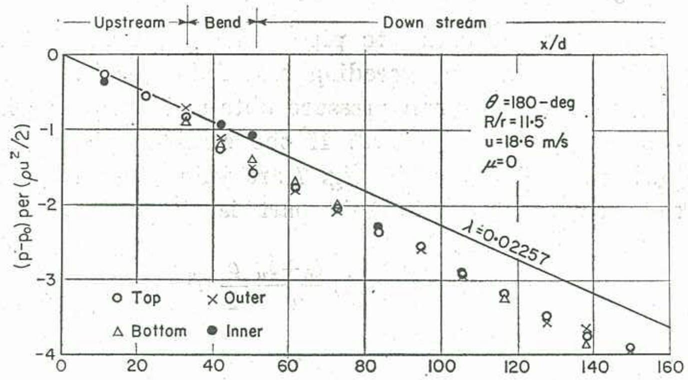

FIG. 5. Pressure distribution along pipe-line.

values $(p - p_0)/(\varrho u^2/2)$ are plotted against the axial length of the pipe expressed in diameter. The distorted flow condition persists for some distance downstream. In the case of $\mu = 0$ the distance of about 50 diameters is necessary before the pressure gradient downstream of the pipe bend becomes constant and presumably the same as that of the upstream tangent.(1) In the case of conveying solids the same distance as that in the case of $\mu = 0$ is necessary, as seen from Fig. 6. The values of λ and $\lambda + \lambda_s$ in Figs. 5 and 6 are obtained from (2) and (9). The differences between the measured values and the straight lines, which represent λ and $\lambda + \lambda_s$, are the

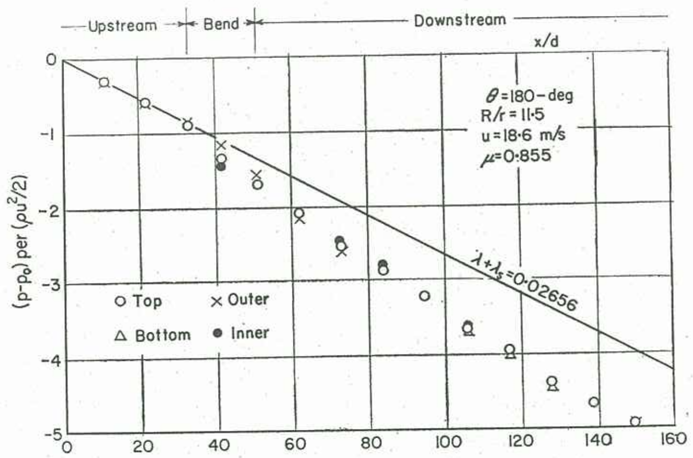

FIG. 6. Pressure distribution along pipe-line.

additional pressure drop due to pipe bend and the effect of pipe bend on the flow in the preceding and following it.

In the following the mean pressure obtained from four holes in the circumference is considered. If the straight pipes preceding and following the pipe bend in Fig. 7 are uninfluenced by the pipe bend, the pressure drop in this part is

$$\Delta p_g' = (\lambda+\lambda_s)\frac{l_0+l_u}{d}\frac{\varrho}{2}u^2 \tag{14}$$

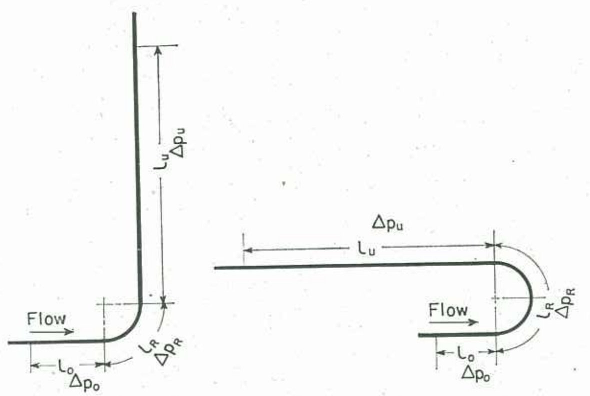

FIG. 7. Explanation of nomenclature.

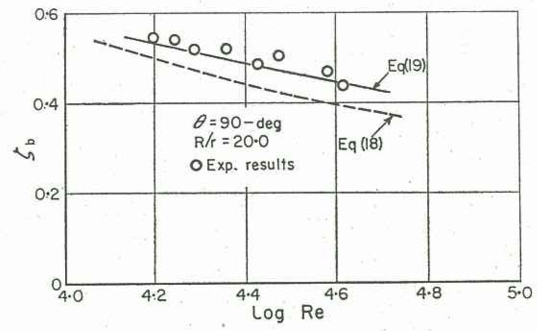

FIG. 8. Relation of ζ_b vs. *Re*.

The effect of the pipe bend is however remarkable. The total pressure drop $\Delta p'$ or the coefficient ζ' is defined by the expressions

$$\Delta p' = \Delta p_0+\Delta p_k+\Delta p_u-\Delta p_g' \tag{15}$$

or

$$\zeta' = \frac{\Delta p'}{\varrho u^2/2} = \frac{\Delta p_0+\Delta p_k+\Delta p_u}{\varrho u^2/2}-(\lambda+\lambda_s)\frac{l_0+l_u}{d} \tag{16}$$

where the assumption is made, that ζ' consists of ζ_b and ζ_s, i.e.

$$\zeta' = \zeta_b+\zeta_s \tag{17}$$

The value of ζ_b obtained from the experimental results are shown plotted against the Reynolds number in Figs. 8 and 9.

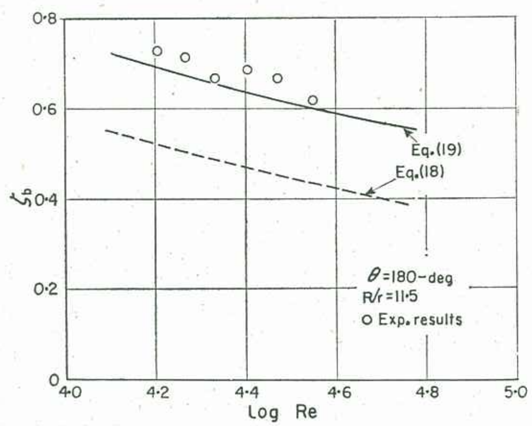

FIG. 9. Relation of ζ_b vs. *Re*.

In these figures the experimental results are compared with two formulae. The one is obtained by Richter[2] in the form

$$\zeta_b = 0{\cdot}00705\ \alpha\theta^{1{\cdot}1}Re^{\beta} \tag{18}$$

where

$$\alpha \fallingdotseq 0{\cdot}48\ R/d, \qquad \beta = -0{\cdot}235$$

and the other is obtained by Itō[3] in the form:

$$\left.\begin{array}{l} \text{For } Re(r/R)^2 < 91 \\ \qquad \zeta_b = 0{\cdot}00873\ \alpha\lambda_c\theta(R/r) \\ \text{for } \quad Re(r/R)^2 > 91 \\ \qquad \zeta_b = 0{\cdot}00241\alpha\theta Re^{-0{\cdot}17}(R/r)^{0{\cdot}84} \end{array}\right\} \tag{19}$$

Approximate expressions for α are:

For $\theta = 90$-deg

$$\left.\begin{array}{ll} \alpha = 0{\cdot}95+17{\cdot}2(R/r)^{-1{\cdot}96}, & R/r < 19{\cdot}7 \\ \text{and} & \\ \alpha = 1, & R/r > 19{\cdot}7 \end{array}\right\} \tag{20}$$

for $\theta = 180$-deg

$$\alpha = 1+116\ (R/r)^{-4{\cdot}52} \tag{21}$$

The values of λ_c in (19) are given from the following equation

$$\lambda_c\left(\frac{R}{r}\right)^{\frac{1}{2}} = \frac{0{\cdot}316}{\{Re(r/R)^2\}^{1/5}} \tag{22}$$

or

$$\lambda_c\left(\frac{R}{r}\right)^{\frac{1}{2}} = 0{\cdot}029+0{\cdot}304\left\{Re\left(\frac{r}{R}\right)^2\right\}^{-0{\cdot}25} \tag{23}$$

Equation (18) gives the coefficient for the pressure drop between the inlet and the exit of pipe bend, while Eq. (19) gives the coefficient for the pressure drop, which consists of both the pressure drop between the inlet and the exit of pipe bend and the effect of pipe bend on the straight pipes preceding and following it. From Figs. 8 and 9, Eq. (19) is applicable as the expression of the first term in the

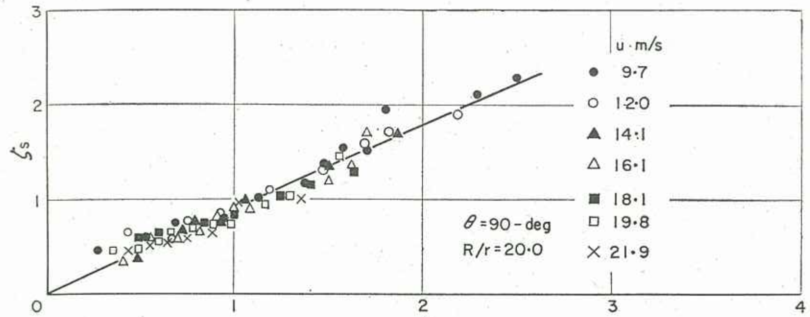

FIG. 10. Relation of ζ_s vs. μ.

right-hand side of Eq. (17). Putting the pressure drop in the case of $\mu = 0$ in the form

$$\Delta p_b = \zeta_b(\varrho u^2/2) \tag{24}$$

the expression for ζ_s is obtained as follows

$$\zeta_s = \frac{\Delta p_0+\Delta p_k+\Delta p_u}{\varrho u^2/2} - (\lambda+\lambda_s)\frac{l_0+l_u}{d} - \frac{\Delta p_b}{\varrho u^2/2} \tag{25}$$

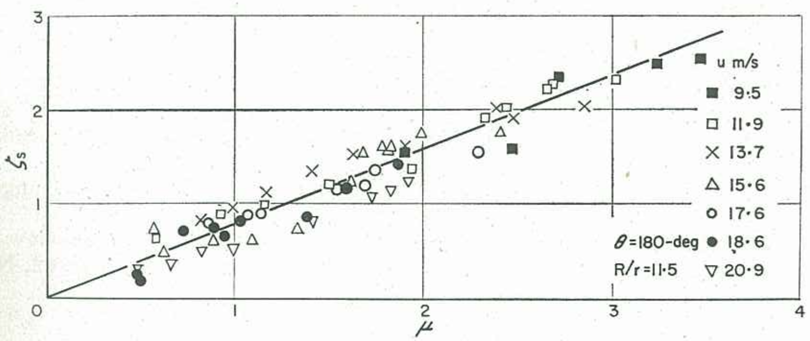

FIG. 11. Relation of ζ_s vs. μ.

The examples of the relation between ζ_s and μ are shown in Figs. 10 and 11. The values a in the expression

$$\zeta_s = a\mu \tag{26}$$

are those in Table 3.

TABLE 3. VALUES OF a

θ deg	R/r	a
90	20·0	0·830
	12·0	0·964
180	19·4	0·747
	11·5	0·771

5. CONCLUSION

In this paper the pressure drop in conveying solids is treated. In both horizontal straight pipe and pipe bend the total pressure drop is separated into the pressure drop due to air only and that due to solids. For the former the known formulae are applicable and for the latter the empirical formulae (12) and (26) are deduced, which give good agreement with experimental results.

REFERENCES

1. ITO, H., Theoretical and experimental investigation concerning the flow through bend pipes, Report 4 (in Japanese), *Memoirs of the Institute of High Speed Mechanics, Tōhoku Univ.* **11,** No. 109 (1955).
2. RICHTER, H., Der Druckabfall in gekrümmten glatten Rohrleitungen *Forsch.-Arb. Ing.-Wesen,* Heft 338 (1930).
3. ITŌ, H., Pressure losses in curved pipes or in pipe bends (A review of some recent advances) (in Japanese), *J. Japan Soc. Mech. Engr.* **62,** No. 490, 1634 (1959).

THE MOTION OF A TWO-DIMENSIONAL BUOYANT VORTEX

I. R. WOOD

Dept. Civil Engineering, University of New South Wales,
Kensington,
NS.W.

Synopsis— In this paper the vortex pair equations are modified by the use of the method of images to include the effects of walls. A quantity of heavy coloured fluid has been released under pressure next to a vertical wall in an experimental rectangular enclosed Perspex flume and a single vortex was obtained. The centre of the resultant intense coloured spot was taken as the vortex centre and its motion between the walls agreed moderately well with that predicted by the modified theory.

The theory for the motion of a single vortex between walls has been modified to allow for a component of the buoyant force acting towards the nearest wall, as occurs with an enclosed flume on a slope. However, for the particular range in which the experiments were conducted, this modification has not been verified due to some of the buoyant fluid escaping from the volume moving with the vortex centre.

The photographic records of each experiment showed the growth of the interface between the coloured and clear fluids as well as the motion of the vortex centre. It is shown that the rate at which the coloured buoyant fluid area grows is proportional to the circulation in the vortex with a constant of proportionality of 0·25. The discovery that entrainment is proportional to the circulation is also consistent with recent measurements on buoyant vortex rings and the value of the constant is of the same order as in the two-dimensional case. The implications of the size of this constant are discussed.

LIST OF SYMBOLS

A	Area of coloured fluid
t	Time
K	Circulation
I	Impulse of a vortex ring, pair or single vortex in the OY direction
y	Distance from the OX axis